Ultrafast Photodynamics of Exciplex Formation and Photoinduced Electron Transfer in Porphyrin−Fullerene Dyads Linked at Close Proximity

Nikolai V. Tkachenko,*,‡ Helge Lemmetyinen,*,‡ Junko Sonoda,† Kei Ohkubo,† Tomoo Sato,⊥ Hiroshi Imahori,*,§ and Shunichi Fukuzumi*,†

Department of Material and Life Science, Graduate School of Engineering, Osaka University, CREST, Japan Science and Technology Corporation, Suita, Osaka 565-0871, Japan, Institute of Materials Chemistry, Tampere University of Technology, P.O. Box 541, FIN-33101 Tampere, Finland, Department of Chemistry, University of Tsukuba, Tsukuba, Ibaraki 305-8571, Japan, and Department of Molecular Engineering, Graduate School of Engineering, Kyoto University, PRESTO, Japan Science and Technology Corporation (JST), Katsura, Nishikyo-ku, Kyoto 615-8510, Japan and Fukui Institute for Fundamental Chemistry, Kyoto University, 34−4, Takano-Nishihiraki-cho, Sakyo-ku, Kyoto 606-8103, Japan

Received: May 22, 2003; In Final Form: August 6, 2003

The ultrafast photodynamics of porphyrin−fullerene dyads in which the distance between the porphyrin and C_{60} moieties is varied systematically at close proximity has been examined using fluorescence up-conversion and pump−probe transient absorption techniques with time resolutions of ca. 100 fs. The porphyrin−fullerene dyads examined are MP-D-C_{60} (M = Zn and 2H) in which the C_{60} moiety is directly connected with the porphyrin ring at the meso position and MP-O-C_{60}, MP-M-C_{60}, and MP-P-C_{60} in which the C_{60} moiety is linked with porphyrin moieties through the benzene ring at the ortho, meta, and para positions, respectively. The charge transfer (CT) bands are observed for MP-D-C_{60} and MP-O-C_{60}, whereas no CT band is seen for MP-M-C_{60} and MP-P-C_{60}. Time-resolved absorption spectral measurements indicate that the photoexcitation of ZnP-D-C_{60} in benzonitrile (PhCN) results in formation of the exciplex, which decays to the ground state without forming the charge-separated state. The strong interaction between the ZnP and the C_{60} moieties due to the short linkage distance in ZnP-D-C_{60} as indicated by the observation of the strongest CT band at the ground state results in formation of the exciplex. The energy of the exciplex is lower than that of the charge-separated state even in a polar solvent such as PhCN. In contrast, the photoexcitation of the dyad with longer linkage, ZnP-O-C_{60}, in PhCN results in formation of the charge-separated state via the exciplex formation, which is higher in energy than the charge-separated state. The photodynamics of exciplex formation of porphyrin−C_{60}-linked dyads with a short linkage is characterized by the extremely fast formation rate from the singlet excited states of porphyrins involving both the second and first excited states due to the interaction between the porphyrin and C_{60} moieties, which are placed at close proximity. In the case of MP-D-C_{60}, the exciplex formation from the first singlet excited state of MP occurs at an ultrafast time scale with a time constant of 160 fs and that from the second singlet excited state occurs faster with a time constant less than 50 fs.

Introduction

During the past half-century, the field of electron-transfer chemistry has undergone a remarkable expansion by the detailed analytic theory developed by R. A. Marcus[1] and also by introduction of new technology such as lasers that have expanded the electron-transfer systems that could be studied, extending to ultrafast reactions in even the femtosecond regime.[2−6] Electron transfer plays a pivotal role not only in chemical processes but also in biological redox processes that are essential for life, such as photosynthesis and respiration.[2,7] Extensive efforts have thereby been devoted toward the preparation of electron donor−acceptor linked-compounds to construct efficient photoinduced electron-transfer systems.[8−15] In particular, the combination of porphyrins and fullerenes has been employed to attain long-lived photoinduced charge-separated (CS) states in high quantum yields, as achieved in the photosynthetic reaction center.[14−17] Porphyrins contain an extensively conjugated two-dimensional π system, which is suitable for efficient electron transfer because the uptake or release of electrons results in minimal structural change upon electron transfer.[18] On the other hand, fullerenes contain an extensively conjugated three-dimensional π system, which is also suitable for efficient electron transfer.[14−17,19] Rates of electron transfer of a variety of electron donor−acceptor systems can be well predicted in light of the Marcus theory of electron transfer, once the fundamental electron-transfer properties of electron donors and acceptors such as the one-electron redox potentials and the reorganization energies of electron transfer are determined.[1,20] In these cases, the interaction between the donor and acceptor moieties is minimized when the type of electron transfer is classified as an outer-sphere electron transfer.[1,20] When the C_{60} moiety is folded onto the porphyrin

* To whom correspondence should be addressed. E-mail addresses: nikolai.tkachenko@tut.fi; fukuzumi@ap.chem.eng.osaka-u.ac.jp; imahori@scl.kyoto-u.ac.jp; helge.lemmetyinen@tut.fi.
† Osaka University.
‡ Tampere University of Technology.
⊥ University of Tsukuba.
§ Kyoto University.

10.1021/jp035412j CCC: $25.00
Published on Web 09/25/2003

CHART 1

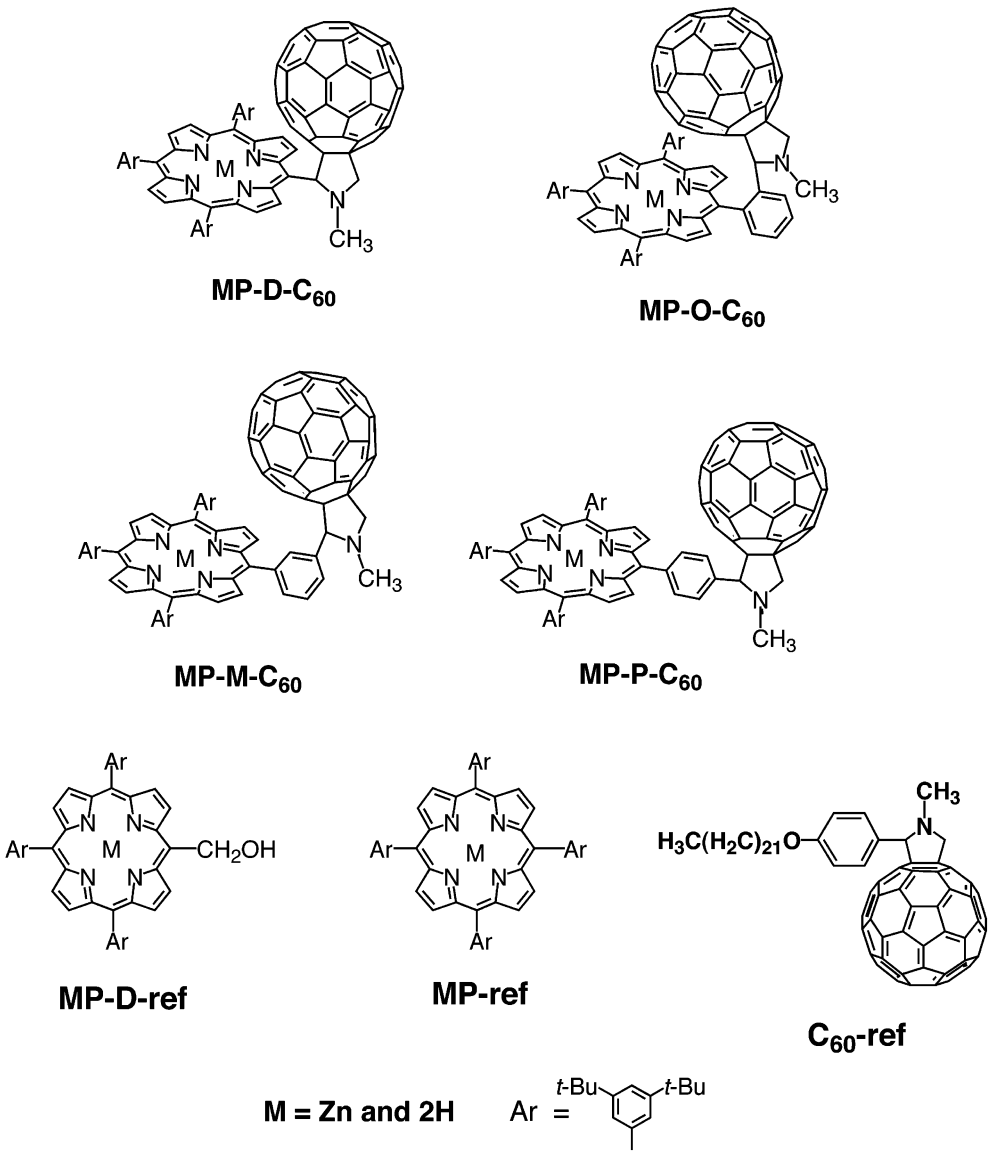

plane, the distance between the C_{60} and the porphyrin moieties (ZnP-O_{34}-C_{60} center-to-center distance (R_{cc}) = 7.6 Å) is close enough to observe the charge-transfer (CT) interaction at both the ground and excited state as indicated by the CT absorption and emission bands,[21] which are not observed for other porphyrin−fullerene dyads in which the porphyrin and the C_{60} were separated apart in longer distances (R_{cc} = 18.6, 14.4, and 12.5 Å).[22] This indicates that the close contact between the porphyrin plane and the C_{60} moiety is essential for the observation of the CT absorption and emission bands.

There have been a number of examples in which charge-transfer excitation of electron donor−acceptor (EDA) complexes resulted in formation of exciplexes, which exhibit high degrees of charge transfer similar to the radical ion pairs.[23−25] The radical ion pair is also formed by electron-transfer quenching of the excited state of an electron donor or acceptor molecule in the EDA complex.[23−25] The important difference between the exciplex formed by charge-transfer excitation and the radical ion pair formed by electron-transfer quenching is their relaxation dynamics.[26] The back electron transfer in the exciplex is generally much faster than that in the radical ion pair formed by electron-transfer quenching of the excited state because of the stronger interaction between the donor and acceptor moieties in the exciplex.[26]

In contrast to such extensive studies on intermolecular formation of exciplexes and radical ion pairs, there have been few studies on intramolecular formation of exciplexes in comparison with the electron-transfer quenching of the excited states in donor−acceptor linked systems.[27] The ultrafast photodynamics of donor−acceptor-linked dyads including exciplex formation and decay and the relation with the charge-separated state has yet to be scrutinized.[27]

We report herein the first comprehensive study on the ultrafast photodynamics of porphyrin−fullerene dyads in which the distance between the porphyrin and C_{60} moieties is varied systematically. The structures of the porphyrin−fullerene dyads examined in this study are shown in Chart 1, in which the dyads are named as ZnP-D-C_{60}, H_2P-D-C_{60}, ZnP-O-C_{60}, H_2P-O-C_{60}, ZnP-M-C_{60}, H_2P-M-C_{60}, ZnP-P-C_{60}, and H_2P-P-C_{60}. Reference compounds (ZnP-D-ref, H_2P-D-ref, ZnP-ref, H_2P-ref, and C_{60}-ref) are also given in Chart 1. In the ZnP-D-C_{60} and H_2P-D-C_{60} dyads, the C_{60} moiety is directly connected with the porphyrin ring at the meso position. The other dyads have the linkage between the C_{60} and porphyrin moieties through the benzene

SCHEME 1

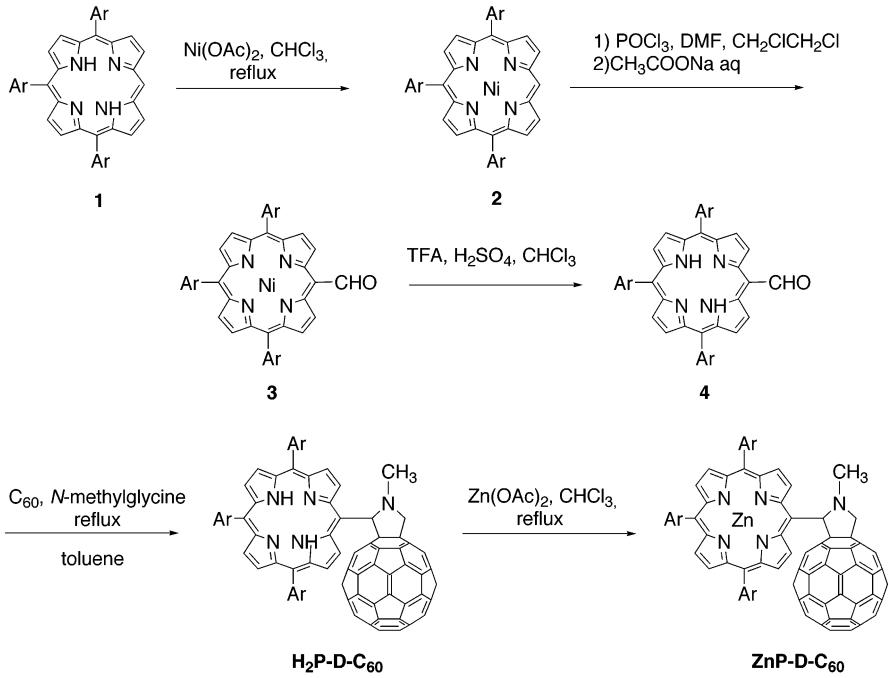

ring at the ortho, meta, and para positions. The photodynamics of ZnP-P-C_{60} and H_2P-P-C_{60} dyads have been reported previously and compared with the results in the present study.[27] The ultrafast dynamics of these porphyrin−fullerene dyads are reported using fluorescence up-conversion and pump−probe transient absorption techniques with time resolutions of ca. 100 fs. The decay-associated spectra, which are employed to reconstruct the sample transient absorption with compensated probe pulse dispersion, allow us to examine the dynamic behavior of the exciplex formation and decay in relation with the dynamics of the formation and decay of the charge-separated state. Thus, the present study provides valuable insight into the relation between the exciplex and the charge-separated state in intramolecular electron transfer in the donor−acceptor linked systems.

Experimental Section

General. Melting points were recorded on a Yanagimoto micro-melting point apparatus and not corrected. ^{1}H NMR spectra were measured on a JEOL JNM-AL300. Matrix-assisted laser desorption/ionization (MALDI) time-of-flight mass spectra (TOF) were measured on a Kratos Compact MALDI I (Shimadzu). Steady-state absorption spectra in the visible and near-IR regions were measured on a Shimadzu UV-3100PC.

Materials. All solvents and chemicals were of reagent grade quality, obtained commercially and used without further purification except as noted below. Tetrabutylammonium hexafluorophosphate used as a supporting electrolyte for the electrochemical measurements was obtained from Tokyo Kasei Organic Chemicals. Benzene, toluene, THF, benzonitrile, and DMF were purchased from Wako Pure Chemical Ind., Ltd., and purified by successive distillation over calcium hydride.[28] Thin-layer chromatography (TLC) and flash column chromatography were performed with Art. 5554 DC-Alufolien Kieselgel 60 F_{254} (Merck), and Fujisilicia BW300, respectively. Preparative-scale size-exclusive chromatography (SEC) was performed using BioRad Bio-Beads SX-1 (Bio-Rad).

Synthesis of MP-D-C_{60}. The synthetic procedures of MP-D-C_{60} are summarized in Scheme 1.

*Compound **1***. A solution of meso-unsubstituted dipyrromethane[29] (2.31 g, 15.8 mmol), 3,5-di-*tert*-butylbenzaldehyde[22] (5.86 g, 26.9 mmol), and 3,5-di-*tert*-butylphenyl-substituted dipyrromethane[30] (4.49 g, 13.41 mmol) in $CHCl_3$ (2200 mL) was degassed by bubbling with nitrogen for 30 min. Then, trifluoroacetic acid was added (3.0 mL, 39.2 mmol). The solution was stirred for 2 h at room temperature under N_2. To the reddish black reaction mixture was added *p*-chloranil (12.4 g, 50.4 mmol), and the resulting mixture was concentrated. Flash column chromatography on silica gel with $CHCl_3$ as the eluent and preparative SEC column chromatography with toluene as the eluent gave **1** as a purple solid (1.56 g, 1.82 mmol, 11.5%). Mp > 300 °C; ^{1}H NMR (300 MHz, $CDCl_3$) δ 10.2 (s, 1H), 9.33 (d, J = 5 Hz, 2H), 9.05 (d, J = 5 Hz, 2H), 8.95 (d, J = 5 Hz, 2H), 8.91 (d, J = 5 Hz, 2H), 8.11 (d, J = 2 Hz, 4H), 8.06 (d, J = 2 Hz, 2H), 1.55 (s, 54H), −2.90 (s, 2H); MALDI-TOFMS (positive mode) m/z 876 ($M + H^+$).

*Compound **2***. A mixture of **1** (1.40 g, 1.60 mmol) and nickel(II) acetate tetrahydrate saturated-methanol solution (20 mL) in $CHCl_3$ (100 mL) was heated at reflux for 20 h. The solution was washed with water, dried over anhydrous sodium sulfate, and filtered, and the solvent was completely removed. Then the residue was passed through short silica gel using $CHCl_3$ eluent. Porphyrin **2** was isolated as a purple-red solid (1.40 g, 1.50 mmol, 94%). Mp > 300 °C; ^{1}H NMR (300 MHz, $CDCl_3$) δ 9.83 (s, 1H), 9.13 (d, J = 5 Hz, 2H), 8.93 (d, J = 5 Hz, 2H), 8.83 (s, 4H), 7.89 (dd, J = 7 Hz, J = 2 Hz, 6H), 7.72 (dt, J = 8 Hz, J = 2 Hz, 3H), 1.49 (s, 54H); MALDI-TOFMS (positive mode) m/z 932 ($M + H^+$).

*Compound **3***. $POCl_3$ (12 mL, 128 mmol) was added dropwise to DMF (10.3 mL, 128 mmol) at 0 °C and stirred for 30 min at room temperature. Then, **2** (1.40 g, 1.50 mmol) in 1,2-dichloroethane (470 mL) was poured at 60 °C and stirred for 1 h. Sodium acetate aqueous solution was added dropwise to the mixture and stirred for 2 h. The reaction mixture was extracted with $CHCl_3$. The organic phase was washed with water and dried over Na_2SO_4. After evaporation, the residue was purified

by column chromatography (SiO_2, 30% $CHCl_3$/hexane) to give **3** as a purple-red solid (1.10 g, 1.15 mmol, 76%). Mp > 300 °C; ^{1}H NMR (300 MHz, $CDCl_3$/DMSO = 5:2) δ 12.0 (s, 1H), 9.79 (d, J = 5 Hz, 2H), 8.88 (d, J = 5 Hz, 2H), 8.69 (d, J = 5 Hz, 2H), 8.62 (d, J = 5 Hz, 2H), 7.80 (d, J = 1 Hz, 6H), 7.71 (dt, J = 8 Hz, J = 2 Hz, 3H), 1.47 (s, 54H); MALDI-TOFMS (positive mode) m/z 960 ($M + H^+$).

*Compound **4***. A solution **3** (1.00 g, 1.04 mmol) in concentrated sulfuric acid (98%, 10 mL) and TFA (10 mL) was stirred for 30 min. Then $NaHCO_3$(aq) (0.1 M) was poured onto the solution at 0 °C. The resulting mixture was poured into $CHCl_3$ (100 mL), and the organic phase was separated. The organic layer was washed with water, dried over anhydrous sodium sulfate, and filtered, and the solvent was removed. The residue was purified by column chromatography over silica using a benzene−hexane mixture (1:2) as an eluent to give **4** as a purple solid (0.75 g, 0.831 mmol, 80%). Mp > 300 °C; ^{1}H NMR (300 MHz, $CDCl_3$) δ 12.51 (s, 1H), 10.01 (d, J = 5 Hz, 2H), 9.00 (d, J = 5 Hz, 2H), 8.80 (d, J = 5 Hz, 2H), 8.73 (d, J = 5 Hz, 2H), 8.02 (dd, J = 6 Hz, J = 2 Hz, 6H), 7.81 (dt, J = 9 Hz, J = 2 Hz, 3H), 1.53 (s, 54H), −1.83 (s, 2H); MALDI-TOFMS (positive mode) m/z 904 ($M + H^+$).

H_2P-D-C_{60}. Porphyrin-linked fullerene H_2P-D-C_{60} was obtained by the 1,3-dipolar cycloaddition of azomethine ylide to fullerene. A mixture of **4** (133 mg, 0.13 mmol), fullerene (0.74 g, 7 equiv), and *N*-methylglycine (0.91 g, 60 equiv) in dry toluene (80 mL) was stirred for 30 min under N_2 and heated at reflux for 70 h. After evaporation, the residue was purified by column chromatography over silica using a benzene−hexane mixture (1:1) as an eluent to give H_2P-D-C_{60} as a dark violet solid (46 mg, 0.0279 mmol, 20%). Mp > 300 °C; ^{1}H NMR (300 MHz, $CDCl_3$) δ 11.58 (d, J = 5 Hz, 1H), 9.92 (d, J = 5 Hz, 1H), 8.96 (d, J = 5 Hz, 1H), 8.93 (d, J = 5 Hz, 1H), 8.88 (d, J = 5 Hz, 1H), 8.84 (d, J = 5 Hz, 1H), 8.82 (d, J = 5 Hz, 1H), 8.78 (d, J = 5 Hz, 1H), 8.13 (s, 1H), 8.05 (s, 1H), 8.05 (s, 1H), 8.03 (s, 1H), 7.99 (s, 1H), 7.81 (s, 2H), 7.78 (t, J = 2 Hz, 1H), 7.78 (t, J = 2 Hz, 1H), 7.75 (t, J = 2 Hz, 1H), 5.55 (d, J = 10 Hz, 1H), 4.85 (d, J = 10 Hz, 1H), 3.13 (s, 3H), 1.56 (s, 9H), 1.53 (s, 9H), 1.50 (s, 18H), 1.49 (s, 18H), −2.53 (s, 2H); MALDI-TOFMS (positive mode) m/z 1653 ($M + H^+$).

ZnP-D-C_{60}. A saturated methanol solution of $Zn(OAc)_2$ (10 mL) was added to a solution of H_2P-D-C_{60} (20 mg, 0.012 mmol) in $CHCl_3$ (50 mL) and refluxed for 12 h. After cooling, the reaction mixture was washed with water twice and dried over anhydrous Na_2SO_4, and then the solvent was evaporated. Flash column chromatography on silica gel with $CHCl_3$ as an eluent and subsequent reprecipitation from chloroform−methanol gave ZnP-D-C_{60} as a dark violet solid (98% yield, 20 mg, 0.012 mmol). Mp > 300 °C; ^{1}H NMR (300 MHz, $CDCl_3$) δ 11.80 (d, J = 5 Hz, 1H), 10.13 (d, J = 5 Hz, 1H), 9.11 (d, J = 5 Hz, 1H), 9.06 (d, J = 5 Hz, 1H), 8.96 (d, J = 5 Hz, 1H), 8.94 (d, J = 5 Hz, 1H), 8.84 (d, J = 5 Hz, 1H), 8.83 (d, J = 5 Hz, 1H), 8.15 (s, 1H), 8.07 (s, 1H), 8.06 (s, 1H), 8.01 (s, 2H), 7.92 (s, 1H), 7.80 (s, 1H), 7.80 (t, J = 2 Hz, 1H), 7.80 (t, J = 2 Hz, 1H), 7.80 (t, J = 2 Hz, 1H), 5.55 (d, J = 10 Hz, 1H), 4.86 (d, J = 10 Hz, 1H), 3.13 (s, 3H), 1.54 (s, 18H), 1.51 (s, 18H), 1.51 (s, 18H); MALDI-TOFMS (positive mode) m/z 1715 ($M + H^+$).

MP-O-C_{60} and MP-M-C_{60} and Reference Compounds. The synthetic procedures and characterization of MP-O-C_{60}, MP-M-C_{60},[27] and MP-D-ref (MP = ZnP or H_2P) are given in Supporting Information. ZnP-ref,[31] H_2P-ref,[31] and C_{60}-ref[17] were prepared by following the same procedures as described previously.

Spectral Measurements. Steady-state fluorescence spectra were measured on a Fluorolog 3 spectrofluorimeter (ISA Inc.) equipped with a cooled IR-sensitive photomultiplier (R2658, Hamamatsu Inc.). The excitation wavelength was at the maximum of the Soret band (410−430 nm region). The emission spectra were recorded in the wavelength range from 600 to 1000 nm with the detection monochromator slits set to 2 nm and the accumulation time set to 1 s. The background counts were subtracted, and the spectra were corrected using the correction function supplied with the instrument (accounting for both photomultiplier quantum efficiency and monochromator throughput spectra). Ultrafast fluorescence decays were measured by an up-conversion method as described previously.[32] The instrument (FOG100, CDP, Moscow, Russia) utilizes the second harmonic (420 nm) of 50 fs pulsed Ti:sapphire laser (TiF50, CDP, Moscow, Russia) pumped by an Ar ion laser (Innova 316P, Coherent). The samples were placed into rotating disk-shaped 1 mm cuvettes. Typical time resolution for the instrument was 150 fs (fwhm). Subnanosecond emission decays were studied using a time-correlated single-photon-counting instrument described elsewhere.[32] The excitation wavelength was 590 nm, and the time resolution was ca. 100 ps. Femtosecond to picosecond time-resolved absorption spectra were collected using a pump−probe technique as described elsewhere.[32b] The femtosecond pulses of the Ti:sapphire generator were amplified by using a multipass amplifier (CDP-Avesta, Moscow, Russia) pumped by a second harmonic of the Nd:YAG Q-switched laser (model LF114, Solar TII, Minsk, Belorussia). The amplified pulses were used to generate second harmonic (420 nm) for sample excitation (pump beam) and white continuum for time-resolved spectrum detection (probe beam). The samples were placed into 1 mm rotating cuvettes, and averaging of 100 pulsed at 10 Hz repetition rate was used to improve signal-to-noise ratio. The wavelength range for a single measurement was 227 nm, and typically three regions were studied, 450−670, 550−780, and 820−1050 nm. Typical response time of the instrument was 150 fs (fwhm). A global multiexponential fitting procedure was applied to process the data. The procedure takes into account the instrument time response function and the group velocity dispersion of the white continuum and allowed calculation of the decay time constants and dispersion-compensated transient absorption spectra.

Electrochemical Measurements. The differential pulse voltammetry measurements were performed on a BAS 50W electrochemical analyzer in a deaerated PhCN solution containing 0.10 M *n*-Bu_4NPF_6 as a supporting electrolyte at 298 K (10 mV s^{-1}). The platinum working electrode was polished with BAS polishing alumina suspension and rinsed with acetone before use. The counter electrode was a platinum wire. The measured potentials were recorded with respect to a $Ag/AgNO_3$ (0.01 M) reference electrode. Ferrocene/ferricenium was used as an external standard. All potentials (vs Ag/Ag^+) were converted to values vs SCE by adding 0.29 V.[33] All electrochemical measurements were carried out under an atmospheric pressure of argon.

Theoretical Calculations. Theoretical calculations were performed on a COMPAQ DS20E computer. The PM3 Hamiltonian was used for the semiempirical MO calculations.[34] Final geometries and energetics were obtained by optimizing the total molecular energy with respect to all structural variables. The heats of formation (ΔH_f) were calculated with the restricted Hartree−Fock (RHF) formalism.

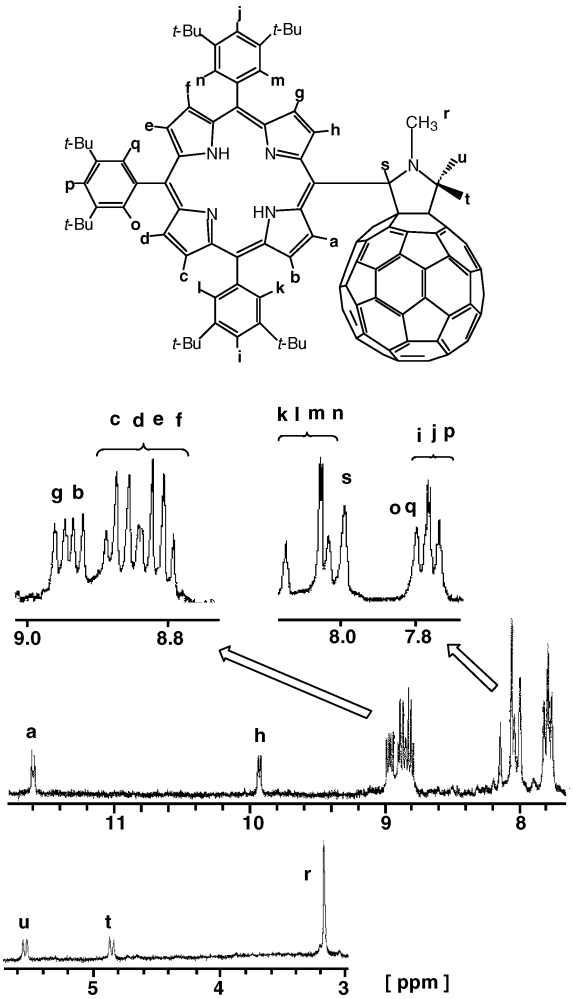

Figure 1. ^{1}H NMR spectrum (300 Hz) of H_2P-D-C_{60} in $CDCl_3$ at room temperature.

Results and Discussion

Ground-State Interaction between Porphyrin and C_{60} in Dyads. The synthesized dyads were well-characterized by spectroscopic analysis including ^{1}H NMR and MALDI-TOF mass spectra (see Experimental Section). The ^{1}H NMR spectrum of H_2P-D-C_{60} shows that all eight β protons are magnetically unequivalent and two of them are shifted to downfield as shown in Figure 1. These two doublets (a and h in Figure 1) can be assigned to the β protons vicinal to the meso carbon connected to the pyrrolidine ring. The large downfield shifts for the two of eight β protons are due to the deshielding effect that results from C_{60} π-electrons. The methyne proton of the pyrrolidine ring (s in Figure 1) also exhibits a downfield shift by about 2 ppm with respect to those of the usual pyrrolidine ring owing to the ring current effect of the porphyrin.

All dyads were studied in two solvents: toluene and benzonitrile. In ZnP-M-C_{60}, H_2P-M-C_{60}, ZnP-P-C_{60}, and H_2P-P-C_{60}, the absorption spectra of the dyads are well reproduced as a sum of the spectra of two chromophores: porphyrin and fullerene. This indicates that there are no observable ground-state interactions between the chromophores.

In contrast, a considerable ground-state interaction of the porphyrin and fullerene moieties is seen in the absorption spectrum of ZnP-D-C_{60} and ZnP-O-C_{60} in nonpolar solvents. The same phenomenon was reported for the zinc derivative of the dyad ZnP-O_{34}-C_{60}, in which the ZnP and the C_{60} moieties are in close proximity (R_{cc} = 7.6 Å).[17] The absorption spectrum

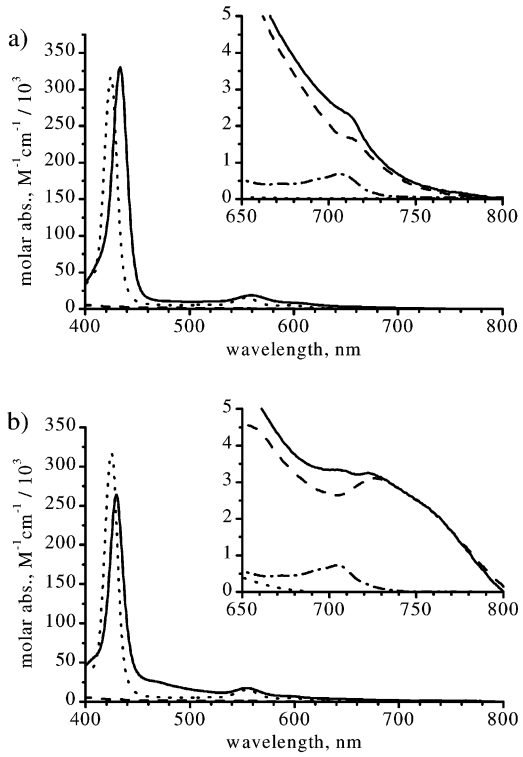

Figure 2. Absorption spectra (a) of ZnP-D-C_{60} (solid line), C_{60}-ref (dashed line), and ZnP-D-ref (dotted line) in benzene (the CT absorption (dash−dotted line) of ZnP-D-C_{60} has been obtained by subtracting the absorptions of ZnP-D-ref and C_{60}-ref from the dyad absorption) and (b) of ZnP-O-C_{60} (solid line), C_{60}-ref (dashed line), and ZnP-ref (dotted line) in toluene (the CT absorption (dash−dotted line) of ZnP-O-C_{60} has been obtained by subtracting the absorptions of ZnP-ref and C_{60}-ref from the dyad absorption).

of ZnP-D-C_{60} is broader and the Soret band is red-shifted as compared with that of the ZnP-D-ref reference porphyrin as shown in Figure 2. Enlarged absorption spectra (650−800 nm) of ZnP-D-C_{60}, ZnP-O-C_{60}, and the reference compounds (ZnP-D-ref, ZnP-ref, and C_{60}-ref) in nonpolar solvents are shown in insets of Figure 2, in which the CT absorption spectra are obtained by subtracting the spectra of porphyrin reference and fullerene reference from those of porphyrin−fullerene dyads. Thus, the ground-state interaction is observed for ZnP-D-C_{60} and ZnP-O-C_{60}, whereas no such interaction is detectable for ZnP-M-C_{60} and ZnP-P-C_{60}. This is ascribed to the shorter distance between the porphyrin and C_{60} moieties for the former cases as compared with the latter.

The calculated structures of H_2P-D-C_{60} and H_2P-O-C_{60} are shown in Figure 3 for comparison. The center-to-center distance between the porphyrin and the C_{60} moieties increases in the order: H_2P-D-C_{60} (8.9 Å) < H_2P-O-C_{60} (9.7 Å) < H_2P-M-C_{60} (10.9 Å) < H_2P-P-C_{60} (12.6 Å).

Excited-State Interaction between Porphyrin and C_{60} in Dyads. The excited-state interaction between porphyrin and C_{60} is expected to be the strongest for ZnP-D-C_{60}, as is the case of the ground-state interaction (vide infra). Figure 4 shows the transient absorption component and time-resolved spectra of ZnP-D-C_{60} in toluene. The transient absorption spectra show broad and featureless absorption bands in the 600−800 nm region extending over 1000 nm and in time scale ranging from the resolution limit of the instrument (∼100 fs) to 1 ns (the longest delay available). Such broad and featureless absorption bands extending over 1000 nm are characteristic of the exciplex in which the porphyrin excited state forms the complex with the C_{60} moiety.[27] The first detected state has lifetime of ∼300

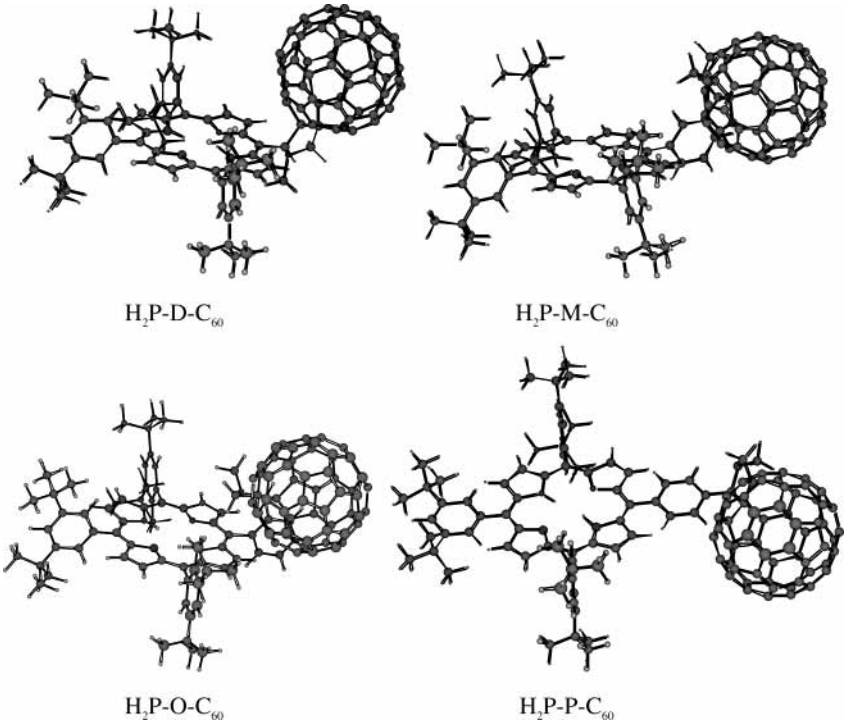

Figure 3. Structures of H_2P-D-C_{60}, H_2P-O-C_{60}, H_2P-M-C_{60}, and H_2P-P-C_{60} obtained by the PM3 calculations. The center-to-center distances (edge-to-edge distances), R_{cc} (R_{ee}), of H_2P-D-C_{60}, H_2P-O-C_{60}, H_2P-M-C_{60}, and H_2P-P-C_{60} are 8.9 (2.6), 9.7 (3.4), 10.9 (3.7), and 12.6 Å (5.2 Å), respectively.

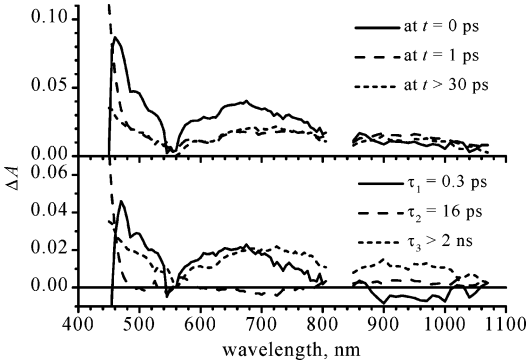

Figure 4. Transient absorption component spectra of ZnP-D-C_{60} in toluene obtained from global three-exponential fit of the data (bottom) and corresponding reconstructed time-resolved spectra (top). The fitted time constants and selected delay times are indicated on the plots.

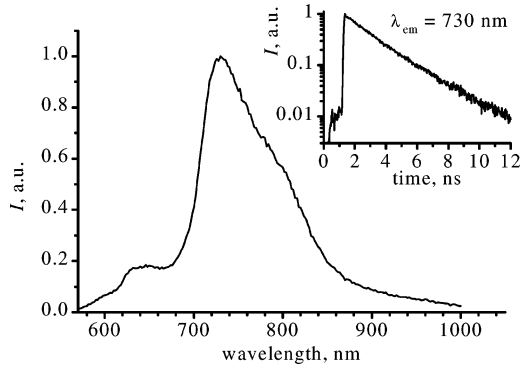

Figure 5. Steady-state emission spectrum of ZnP-D-C_{60} in toluene. Inset shows the emission decay at 730 nm (the major decay lifetime is 1.6 ns).

fs and will be discussed later. The second decay component, 16 ps, has only minor impact on the absorption spectrum in visible and IR regions. Overall lifetime of the exciplex is longer than the time scale measured, that is, >1 ns.

The exciplex emission of ZnP-D-C_{60} in toluene is observed as a steady-state emission at $\lambda_{max} = 730$ nm when excited at 430 nm as shown in Figure 5. Subnanosecond emission decays were measured using a time-correlated single-photon-counting instrument (see Experimental Section). At wavelengths longer than 720 nm, the decay profiles were almost monoexponential with dominating time constant of 1.6 ns (as shown in the inset of Figure 5), which is the exciplex lifetime for ZnP-D-C_{60} in toluene.

In a much more polar solvent (PhCN) than toluene, virtually the same transient absorption spectra are obtained as the case in toluene (compare the spectra in Figure 6 with those in Figure 4). The broad and featureless absorption bands in the 600−800 nm region extending over 1000 nm, which are characteristic of the exciplex, are also observed in Figure 6, and no sharp absorption band at 640 nm[35,36] due to $ZnP^{\bullet+}$ is detected.

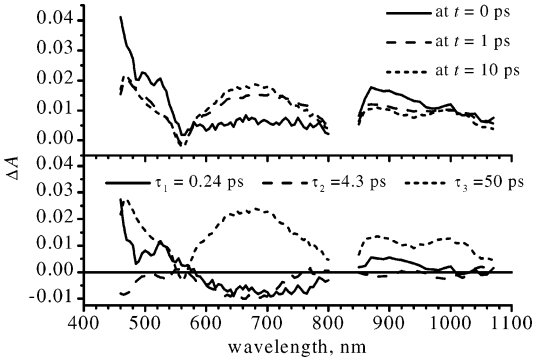

Figure 6. Transient absorption component spectra of ZnP-D-C_{60} in PhCN obtained from global three-exponential fit of the data (bottom) and corresponding reconstructed time-resolved spectra (top). The fitted time constants and selected delay times are indicated on the plots.

The dynamics of the exciplex formation and decay at 690 nm is shown in Figure 7. The initial instantaneous rise (0−0.2 ps) is followed by a slower rise (0.5−5 ps), as seen in the inset of Figure 7. The initial fast formation of the exciplex is

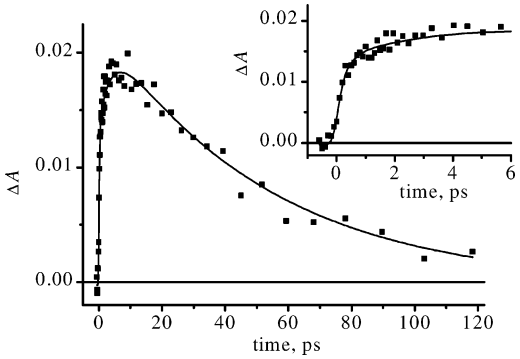

Figure 7. Transient absorption time profile for ZnP-D-C_{60} in PhCN at 690 nm, which shows formation and decay of the exciplex.

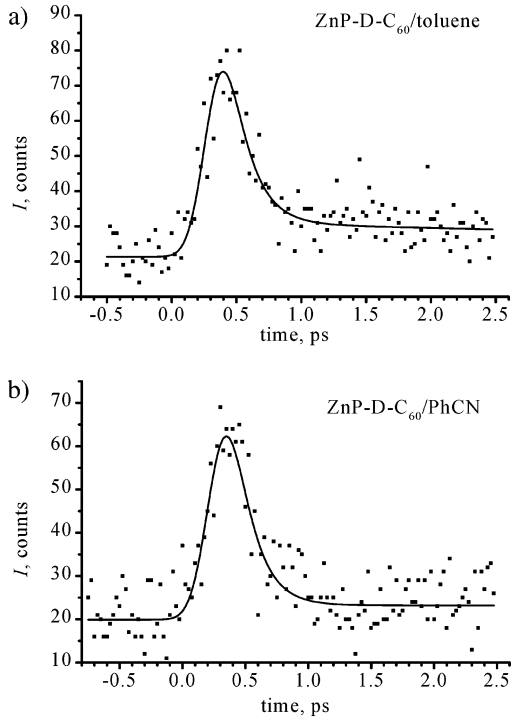

Figure 8. Porphyrin fluorescence decays at 600 nm for ZnP-D-C_{60} in (a) toluene and (b) PhCN measured by up-conversion method (dots). The solid lines show fits of the data with decay time of 160 fs and instrument response time of 150 fs.

consistent with the fast emission decay of the porphyrin locally excited singlet state of ZnP-D-C_{60} in PhCN (lifetime of 160 fs) measured by the up-conversion method (Figure 8). The exciplex decays with a lifetime of 50 ps to the ground state (Figure 7), which is much shorter than that in toluene.

The primary excited state of ZnP-D-C_{60} is the second singlet excited state of ZnP (^{2S}ZnP*-D-C_{60}).[37−39] The internal conversion of the second singlet excited state to the first singlet excited state is known to occur on a time scale of 1 ps,[3b,37−39] which is certainly much slower than the fast emission rise and decay of the ^{1S}ZnP* fluorescence in Figure 8 (160 fs). This indicates that the ^{2S}ZnP*-D-C_{60} state is relaxed to the exciplex (ZnP-D-C_{60})* in competition to the first singlet excited state (^{1S}ZnP*-D-C_{60}), which is also converted to the exciplex. The energy transfer from ^{1S}ZnP* may also occur to the C_{60} moiety to produce (ZnP-D-$^{1S}C_{60}$*).[27] The subsequent slower rise in the absorption due to the exciplex is thereby ascribed to the exciplex formation from ZnP-D-$^{1S}C_{60}$*.[40] In addition, the instant appearance of the exciplex upon photoexcitation (most pronounced in toluene, see time-resolved spectrum at $t = 0$ ps, Figure 4) indicates that the exciplex is also formed from the second excited

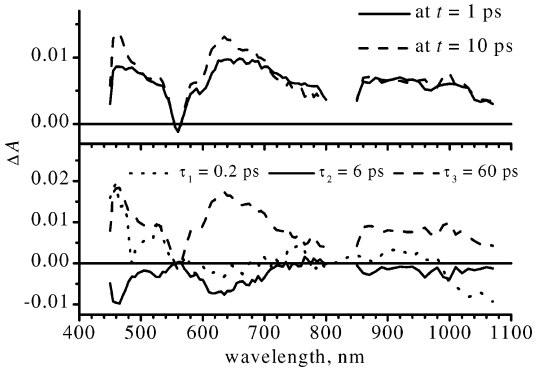

Figure 9. Transient absorption component spectra of ZnP-O-C_{60} in PhCN obtained from global three-exponential fit of the data (bottom) and corresponding reconstructed time-resolved spectra (top). The fitted time constants and selected delay times are indicated on the plots.

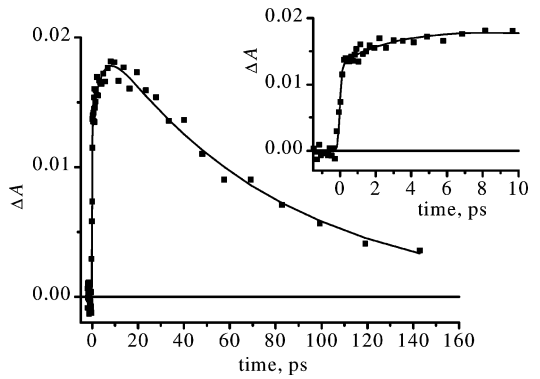

Figure 10. Transient absorption time profile for ZnP-O-C_{60} in PhCN at 630 nm.

SCHEME 2

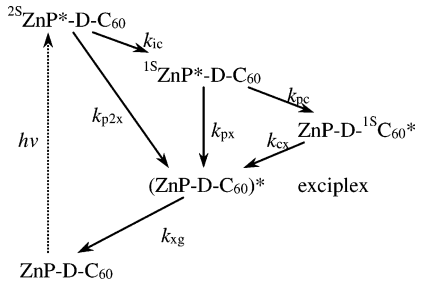

state of ZnP (^{2S}ZnP*-D-C_{60}), because the direct photoexcitation of the CT band of ZnP-D-C_{60} is highly unlikely because of the much smaller CT absorption than the Soret band at the excitation wavelength (415 nm).[41] The photodynamics of the exciplex formation and decay is summarized in Scheme 2.

A slight elongation of the distance between the ZnP and C_{60} moieties in the dyad results in a change in the energy balance between the exciplex and the charge-separated state. The transient absorption spectra of ZnP-O-C_{60} in PhCN are shown in Figure 9, in which the sharp absorption band at 640 nm due to the $ZnP^{\bullet+}$ moiety is observed together with the absorption band at 1000 nm[42−44] due to the $C_{60}^{\bullet-}$ for the component that has the longest lifetime (60 ps). It is worthy of notice that the transient absorption spectra of ZnP-O-C_{60} and ZnP-D-C_{60} at a short delay time (compare spectra at $t = 1$ ps in Figures 6 and 9) are virtually identical to each other. The difference in spectra appears at the completion of the picosecond processes, when the charge-separated state of ZnP-O-C_{60} is formed.

The time profile of the absorbance at 630 nm is shown in Figure 10. The initial instant rise (0−0.2 ps) is followed by a

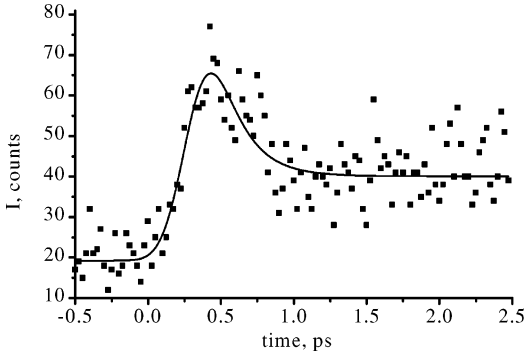

Figure 11. Fluorescence decay of ZnP-O-C_{60} in PhCN measured with up-conversion method (dots). The solid line shows a fit of the data where the fast decay lifetime is 180 fs and the instrument response time is 160 fs.

SCHEME 3

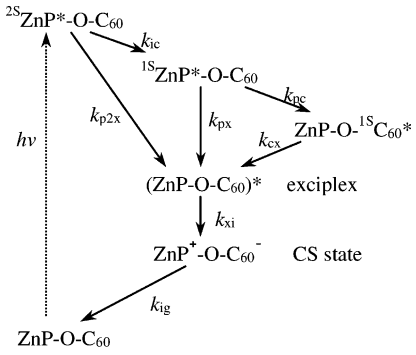

slower rise ($\tau_2 = 6$ ps), as seen in the inset of Figure 10. The transient absorption spectrum at 1 ps delay (Figure 9) indicates that at this time the exciplex is already formed. The initial ultrafast formation of the exciplex is consistent with the ultrafast emission decay of ZnP-O-C_{60} in PhCN (lifetime of 180 fs) measured by the up-conversion method (Figure 11). The mirror image between the decay component spectra of 6 and 60 ps in Figure 9 indicates that the charge-separated state (ZnP$^{\bullet+}$-O-$C_{60}^{\bullet-}$) is formed with a time constant of 6 ps and has lifetime of 60 ps.

The photodynamics of ZnP-O-C_{60} in PhCN is summarized in Scheme 3. The second singlet excited state is formed upon photoexcitation and is relaxed to the exciplex and the first singlet excited state, which is also converted to the exciplex with the lifetime of 180 fs. The exciplex formation from the second singlet excited state occurs within instrumental resolution ($<$50 fs). The exciplex is then converted to the charge-separated state with the time constant of 6 ps. The charge-separated state decays to the ground state with the lifetime of 60 ps.

When benzonitrile is replaced by toluene, the charge-separated state is not observed any more and instead only the exciplex is formed, as shown in Figure 12, in which the transient absorption component spectra of ZnP-O-C_{60} in toluene have only broad and featureless absorption bands in the 600−800 nm region extending over 1000 nm, which are characteristic of the exciplex. The transient absorption spectra of ZnP-D-C_{60} and ZnP-O-C_{60} in toluene are very much alike, and the photodynamics of ZnP-O-C_{60} can be well presented by Scheme 2.

Further elongation of the distance between the donor and acceptor results in a further stabilization of the charge-separated state relative to the exciplex. The transient absorption measurements of ZnP-M-C_{60} in PhCN (Figure 13) show all key features observed for ZnP-O-C_{60} in PhCN (Figure 9), but the time constants of the reactions are gradually increased. The lifetime

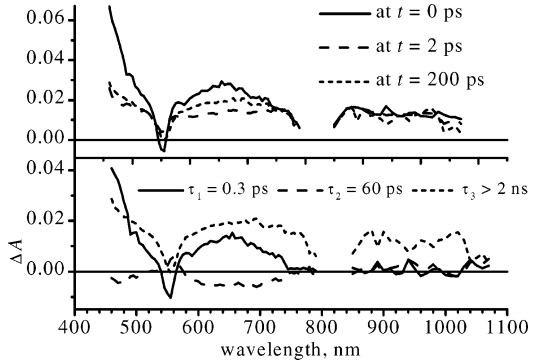

Figure 12. Transient absorption component spectra of ZnP-O-C_{60} in toluene obtained from global three-exponential fit of the data (bottom) and corresponding reconstructed time-resolved spectra (top).

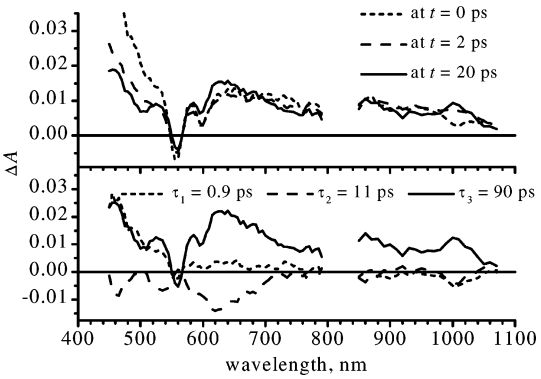

Figure 13. Transient absorption component spectra of ZnP-M-C_{60} in PhCN obtained from global three-exponential fit of the data (bottom) and corresponding reconstructed time-resolved spectra (top).

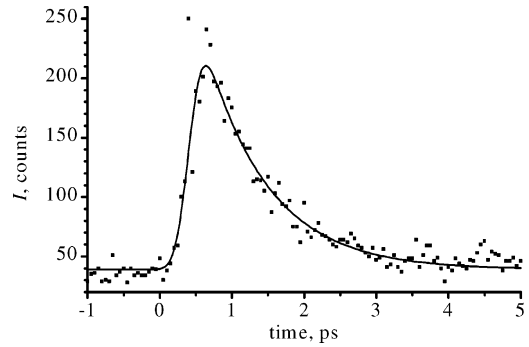

Figure 14. Fluorescence decay of ZnP-M-C_{60} in PhCN measured with up-conversion method (dots). The solid line shows a monoexponential fit of the data with time constant of 0.9 ± 0.2 ps (the instrument response time is 160 fs).

of the charge-separated state is 90 ps, and the time constant for the transition from exciplex to charge-separated state is 11 ps. Also the lifetime of the singlet excited state of porphyrin chromophore is 0.9 ps for ZnP-M-C_{60}, as indicated by up-conversion measurements (Figure 14). In contrast to the results in PhCN, only a long-lived exciplex was observed for ZnP-M-C_{60} in toluene, similar to that of ZnP-O-C_{60} and ZnP-D-C_{60} (see Supporting Information).

ZnP-P-C_{60} dyad studied previously fits perfectly well into the observed tendency in this study.[27] In PhCN, the charge-separated state is formed via the exciplex, that is, the energy of the charge-separated state is lower than that of the exciplex, whereas in toluene only the exciplex was observed. Also the time constants of the reactions are the slowest for ZnP-P-C_{60} as compared to other dyads involved in this study.

TABLE 1: Rate Constants for Exciplex Formation and Decay and Decay Rate Constants of Charge-Separated States (When Observed)[a]

dyad	solvent	k_{p2x},[b] s^{-1}	k_{px},[c] s^{-1}	k_{cx}, s^{-1}	k_{xg}, s^{-1}	k_{xi}, s^{-1}	k_{ig}, s^{-1}
ZnP-D-C_{60}	toluene	$\geq 2 \times 10^{13}$	$\sim 6 \times 10^{12}$	6.3×10^{10}	0.6×10^{9}		
	PhCN	$\geq 2 \times 10^{13}$	$\sim 7 \times 10^{12}$	2.3×10^{11}	2×10^{10}		
ZnP-O-C_{60}	toluene	$\geq 2 \times 10^{13}$	$\sim 6 \times 10^{12}$	1.7×10^{10}	6.3×10^{8}		
	PhCN	$\geq 2 \times 10^{13}$	$\sim 6 \times 10^{12}$			1.7×10^{11}	1.7×10^{10}
ZnP-M-C_{60}	toluene		1.1×10^{12}	$\sim 3 \times 10^{10}$	6.3×10^{8}		
	PhCN		1.1×10^{12}			9.1×10^{10}	1.1×10^{10}
ZnP-P-C_{60}	toluene		5×10^{11}		7.7×10^{8}		
	PhCN		5×10^{11}			8.3×10^{10}	7.7×10^{9}
H_2P-D-C_{60}	toluene		5×10^{12}		6×10^{8}		
	PhCN		5×10^{12}	$\sim 5 \times 10^{10}$	5×10^{9}		
H_2P-O-C_{60}	toluene		5×10^{12}				
	PhCN		7×10^{12}			4×10^{10}	2.9×10^{9}
H_2P-M-C_{60}	toluene		1.3×10^{11}		$\sim 10^{10}$ [d]		
	PhCN		1×10^{11}			1.5×10^{10}	1.1×10^{9}
H_2P-P-C_{60}	toluene		3×10^{10}		4×10^{9} [d]		
	PhCN[e]						1.1×10^{9}

[a] The rate constants are marked according to notation used in Schemes 2 and 3. [b] Two pathways contribute to the relaxation of the second excited state: internal conversion (k_{ic}) and exciplex formation (k_{p2x}). Assuming $k_{ic} \approx 10^{12}$ s^{-1},[37-39] the fast component is mainly due to exciplex formation. [c] A competing process is intermolecular energy transfer (k_{pc}), which is a minor relaxation channel and has been neglected in calculations. [d] The exciplex decays to fullerene singlet excited state. [e] Exciplex was not observed.

The observed trends in the exciplex and charge-transfer photodynamics indicate that both the distance between the ZnP and C_{60} moieties and solvent polarity are important in determining the energy balance between the charge-separated state and the exciplex.[45] In the case of ZnP-D-C_{60} in PhCN, the strong interaction between the ZnP and the C_{60} moieties due to the short linkage distance as indicated by the observation of the strongest CT band in the ground state results in lowering the energy of the exciplex, which becomes lower than the charge-separated state even in a polar solvent such as PhCN (Scheme 2). Already in the case of ZnP-O-C_{60}, the interaction in the exciplex is not strong enough to make the energy lower than that of the charge-separated state, which is stabilized by polar solvent molecules (Scheme 3). Virtually the same results are obtained for the dyads with a longer linkage (ZnP-M-C_{60} and ZnP-P-C_{60}), which afford the charge-separated states via the exciplex formation in PhCN. In toluene, the solvent stabilization of the charge-separated state is not as strong as that in PhCN and the charge-separated state becomes higher in energy than the exciplex.

Qualitatively similar tendency was observed for free-base dyads. The transient absorption spectra of H_2P-D-C_{60} and H_2P-O-C_{60} in PhCN are presented in Figure 15. In the case of H_2P-D-C_{60} only a broad and featureless absorption band of the exciplex is seen in the red and infrared regions. In contrast, the transient data for H_2P-O-C_{60} in PhCN shows reshaping of the spectra due to the transition from the exciplex to the charge-separated state. As in the case of zinc porphyrin−C_{60} dyads, the charge-separated state was not observed in toluene for free-base porphyrin−C_{60} dyads. Moreover, for H_2P-P-C_{60} in toluene, there was no direct evidence of exciplex formation,[27] and for H_2P-M-C_{60}, the exciplex energy appeared to be higher than the energy of the singlet excited fullerene chromophore, which resulted in efficient energy transfer from porphyrin to fullerene mediated by the exciplex (see Supporting Information for details). Unlike for zinc porphyrins, internal conversion of the second excited state to the first excited state is faster than 100 fs. Therefore the formation of exciplex directly from the porphyrin second singlet excited state should be relatively inefficient for free-base porphyrin−C_{60} dyads but cannot be excluded totally.

The data of emission decay by the up-conversion methods and transient absorption spectra afford the rate constants of photodynamics of MP-D-C_{60}, MP-O-C_{60}, MP-M-C_{60}, and MP-P-C_{60} dyads (M = Zn and 2H) in PhCN and toluene. The results are summarized in Table 1. The ultrafast formation of the exciplex from the porphyrin second excited state (^{2S}P*) deserves a special comment. This feature is the most pronounced in toluene for ZnP-D-C_{60} and ZnP-O-C_{60} (and their free-base analogues), where transient absorption spectra hold the exciplex character immediately after excitation (spectra at $t = 0$ ps in Figures 4, 12, and 15a). Although for these samples some emission from the porphyrin first singlet excited state was observed, the emission intensity was very weak (e.g., compare Figures 8 and 14) and the lifetime was extremely short (Figures 8 and 11). This means that the quantum yield of the internal

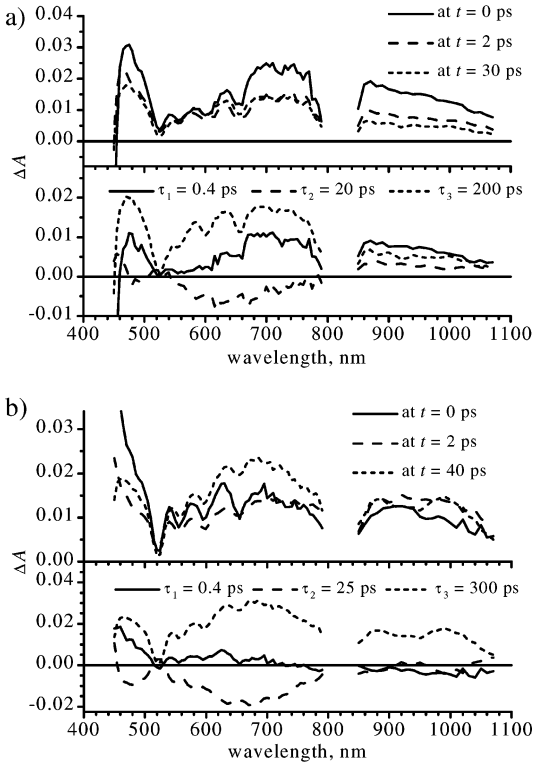

Figure 15. Results of the pump−probe studies of (a) H_2P-D-C_{60} and (b) H_2P-O-C_{60} in PhCN. The lower plots show absorption component spectra obtained from the global three-exponential fits, and the upper plots show corresponding reconstructed time-resolved spectra.

conversion is reduced gradually and there is an alternative pathway for the second excited-state relaxation. This alternative pathway is exciplex formation, as revealed by the transient spectra at $t = 0$ ps (Figures 4 and 12), and because the reaction was not time-resolved in our measurements, its time constant is beyond the time resolution of the instrument; it is shorter than 50 fs.

Another noticeable result is that the rate constants of the exciplex formation from the porphyrin first singlet excited state (k_{px}) are not affected by the solvent polarity but they are very sensitive to the donor−acceptor distance and mutual orientation. In terms of center-to-center distance (R_{cc}), the distance increase by 3 Å (ZnP-O-C_{60} vs ZnP-P-C_{60})[46] results in more than 10-fold decrease in the exciplex formation rate. For comparison, the ratio of the charge recombination rates (k_{ig}) for the same compounds is only 2.2. A similar trend is seen for the free-base porphyrin−C_{60}. This sharp difference in distance dependences for the exciplex and charge-separated state indicates that these two states have rather different electronic configurations, that is, the corresponding electronic coupling matrix elements have very different distance/orientation dependence.

It is interesting to note that in PhCN the lifetimes of the exciplex for ZnP-D-C_{60} and the charge-separated state for ZnP-O-C_{60} are virtually the same: 55 and 60 ps, respectively. ZnP-D-C_{60} is characterized by a shorter DA distance as compared with ZnP-O-C_{60}, and under other equal conditions, the decay rate of the exciplex of ZnP-D-C_{60} is expected to be greater than the charge recombination rate of the charge-separated state of ZnP-O-C_{60}.[47] However, the exciplex results in a smaller reorganization energy as compared to the charge-separated state, and accounting for the fact that the charge recombination takes place in inverted Marcus region, the recombination of a state with greater reorganization energy (the charge-separated state) should be faster than that of the exciplex. In this particular case, these two opposite effects (increase of the rate due to increase in reorganization energy and decrease of the rate due to distance increase) may compensate each other resulting in similar recombination rates.

In conclusion, the photodynamics of exciplex formation of porphyrin−C_{60}-linked dyads is characterized by the extremely fast formation from the singlet excited states of porphyrins involving both the second and first excited states due to the interaction between the porphyrin and C_{60} moieties, which are placed at close proximity. In the case of ZnP-D-C_{60}, which has the shortest linkage, the strong interaction between the ZnP and C_{60} moieties results in lowering the energy of the exciplex, which becomes lower than the charge-separated state even in a polar solvent such as PhCN (Scheme 2).

Acknowledgment. This work was partially supported by Grants-in-Aid for Scientific Research on Priority Area (Grant Nos. 11228205 and 13440216) and Grant-in-Aid for the Development of Innovative Technology (Grant No. 12310) from the Ministry of Education, Culture, Sports, Science and Technology, Japan, and by the Academy of Finland and the National Technology Agency of Finland. H.I. also thanks Grant-in-Aid from the Ministry of Education, Culture, Sports, Science and Technology, Japan (21st Century COE on Kyoto University Alliance for Chemistry) for financial support.

Supporting Information Available: Experimental details including synthetic procedures and characterization, emission and transient absorption spectra, and cyclic voltammetry in benzonitrile. This material is available free of charge via the Internet at http://pubs.acs.org.

References and Notes

(1) (a) Marcus, R. A. *Annu. Rev. Phys. Chem.* **1964**, *15*, 155. (b) Marcus, R. A. *Angew. Chem., Int. Ed. Engl.* **1993**, *32*, 1111. (c) Marcus, R. A.; Sutin, N. *Biochim. Biophys. Acta* **1985**, *811*, 265.

(2) (a) *Electron Transfer in Chemistry*; Balzani, V., Ed.; Wiley-VCH: Weinheim, Germany, 2001. (b) Mataga, N.; Miyasaka, H. *Prog. React. Kinet.* **1994**, *19*, 317. (c) Gauduel, Y. *J. Mol. Liq.* **1995**, *63*, 1. (d) Wynne, K.; Hochstrasser, R. M. *Adv. Chem. Phys.* **1999**, *107*, 263. (e) Zhang, J. Z. *J. Phys. Chem. B* **2000**, *104*, 7239.

(3) (a) Mataga, N.; Miyasaka, H. *Adv. Chem. Phys.* **1999**, *107*, 431. (b) Mataga, N.; Chosrowjan, H.; Shibata, Y.; Yoshida, N.; Osuka, A.; Kikuzawa, T.; Okada, T. *J. Am. Chem. Soc.* **2001**, *123*, 12422.

(4) (a) Chiorboli, C.; Rodgers, M. A. J.; Scandola, F. *J. Am. Chem. Soc.* **2003**, *125*, 483. (b) Reid, G. D.; Whittaker, D. J.; Day, M. A.; Creely, C. M.; Tuite, E. M.; Kelly, J. M.; Beddard, G. S. *J. Am. Chem. Soc.* **2001**, *123*, 6953. (c) Kambhampati, P.; Son, D. H.; Kee, T. W.; Barbara, P. F. *J. Phys. Chem. A* **2000**, *104*, 10637.

(5) (a) Wan, C.; Fiebig, T.; Schiemann, O.; Barton, J. K.; Zewail, A. H. *Proc. Natl. Acad. Sci. U.S.A.* **2000**, *97*, 14052. (b) Kononov, A. I.; Moroshkina, E. B.; Tkachenko, N. V.; Lemmetyinen, H. *J. Phys. Chem. B* **2001**, *105*, 535. (c) Lewis, F. D.; Wu, T.; Liu, X.; Letsinger, R. L.; Greenfield, S. R.; Miller, S. E.; Wasielewski, M. R. *J. Am. Chem. Soc.* **2000**, *122*, 2889.

(6) (a) Asbury, J. B.; Ghosh, H. N.; Ellingson, R. J.; Ferrere, S.; Nozik, A. J.; Lian, T. *Ultrafast Phenomena XI*; Springer Series in Chemical Physics; Springer: Berlin, Germany, 1998; p 639. (b) Asbury, J. B.; Hao, E.; Wang, Y.; Ghosh, H. N.; Lian, T. *J. Phys. Chem. B* **2001**, *105*, 4545. (c) Zimmermann, C.; Willig, F.; Ramakrishna, S.; Burfeindt, B.; Pettinger, B.; Eichberger, R.; Storch, W. *J. Phys. Chem. B* **2001**, *105*, 9245.

(7) Kaim, W.; Schwederski, B. *Bioinorganic Chemistry: Inorganic Elements in the Chemistry of Life*; Wiley: Chichester, U.K., 1994.

(8) (a) Paddon-Row, M. N. *Acc. Chem. Res.* **1994**. *27*, 18. (b) Jordan, K. D.; Paddon-Row, M. N. *Chem. Rev.* **1992**, *92*, 395. (c) Paddon-Row, M. N. In *Electron Transfer in Chemistry*; Balzani, V., Ed.; Wiley-VCH: Weinheim, Germany, 2001; Vol. 3, pp 179−271.

(9) (a) Wasielewski, M. R. In *Photoinduced Electron Transfer*; Fox, M. A., Chanon, M., Eds.; Elsevier: Amsterdam, 1988; Part A, pp 161−206. (b) Wasielewski, M. R. *Chem. Rev.* **1992**, *92*, 435. (c) Wasielewski, M. R.; Wiederrecht, G. P.; Svec, W. A.; Niemczyk, M. P. *Sol. Energy Mater. Sol. Cells* **1995**, *38*, 127.

(10) Verhoeven, J. W. *Adv. Chem. Phys.* **1999**, *106*, 603.

(11) (a) Osuka, A.; Mataga, N.; Okada, T. *Pure Appl. Chem.* **1997**, *69*, 797. (b) Sun, L.; Hammarström, L.; Åkermark, B.; Styring, S. *Chem. Soc. Rev.* **2001**, *30*, 36. (c) Scandola, F.; Chiorboli, C.; Indelli, M. T.; Rampi, M. A. In *Electron Transfer in Chemistry*; Balzani, V., Ed.; Wiley-VCH: Weinheim, Germany, 2001; Vol. 3, pp 337−408.

(12) (a) Harriman, A.; Sauvage, J.-P. *Chem. Soc. Rev.* **1996**, *25*, 41. (b) Blanco, M.-J.; Jiménez, M. C.; Chambron, J.-C.; Heitz, V.; Linke, M.; Sauvage, J.-P. *Chem. Soc. Rev.* **1999**, *28*, 293. (c) Chambron, J. C.; Collin, J. P.; Dalbavie, J. O.; Dietrich-Buchecker, C. O.; Heitz, V.; Odobel, F.; Solladie, N.; Sauvage, J. P. *Coord. Chem. Rev.* **1998**, *180*, 1299.

(13) (a) Lewis, F. D.; Liu, X. Y.; Liu, J. Q.; Miller, S. E.; Wasielewski, M. R. *Nature* **2000**, *406*, 51. (b) Lewis, F. D.; Letsinger, R. L.; Wasielewski, M. R. *Acc. Chem. Res.* **2001**, *34*, 159.

(14) (a) Imahori, H.; Sakata, Y. *Adv. Mater.* **1997**, *9*, 537. (b) Imahori, H.; Sakata, Y. *Eur. J. Org. Chem.* **1999**, *64*, 2445. (c) Fukuzumi, S.; Imahori, H. In *Electron Transfer in Chemistry*; Balzani, V., Ed.; Wiley-VCH: Weinheim, Germany, 2001; Vol. 2, pp 927−975. (d) Imahori, H.; Mori, Y.; Matano, Y. *Photochem. Photobiol. C* **2003**, *4*, 51.

(15) (a) Gust, D.; Moore, T. A. In *The Porphyrin Handbook*; Kadish, K. M., Smith, K. M., Guilard, R., Eds.; Academic Press: San Diego, CA, 2000; Vol. 8, pp 153−190. (b) Gust, D.; Moore, T. A.; Moore, A. L. *Acc. Chem. Res.* **2001**, *34*, 40. (c) Gust, D.; Moore, T. A.; Moore, A. L. In *Electron Transfer in Chemistry*; Balzani, V., Ed.; Wiley-VCH: Weinheim, Germany, 2001; Vol. 3, pp 272−336.

(16) (a) Imahori, H.; Yamada, K.; Hasegawa, M.; Taniguchi, S.; Okada, T.; Sakata, Y. *Angew. Chem., Int. Ed. Engl.* **1997**, *36*, 2626. (b) Imahori, H.; Tamaki, K.; Guldi, D. M.; Luo, C.; Fujitsuka, M.; Ito, O.; Sakata, Y.; Fukuzumi, S. *J. Am. Chem. Soc.* **2001**, *123*, 2607. (c) Fukuzumi, S.; Imahori, H.; Yamada, H.; El-Khouly, M. E.; Fujitsuka, M.; Ito, O.; Guldi, D. M. *J. Am. Chem. Soc.* **2001**, *123*, 2571.

(17) Imahori, H.; Guldi, D. M.; Tamaki, K.; Yoshida, Y.; Luo, C.; Sakata, Y.; Fukuzumi, S. *J. Am. Chem. Soc.* **2001**, *123*, 6617.

(18) Fukuzumi, S. In *The Porphyrin Handbook*; Kadish, K. M., Smith, K. M., Guilard, R., Eds.; Academic Press: San Diego, CA, 2000; Vol. 8, pp 115−151.

(19) (a) Fukuzumi, S.; Guldi, D. M. In *Electron Transfer in Chemistry*; Balzani, V., Ed.; Wiley-VCH: Weinheim, Germany, 2001; Vol. 2, pp 270−337. (b) Guldi, D. M. *Chem. Soc. Rev.* **2002**, *31*, 22.

(20) Eberson, L. *Electron-Transfer Reactions in Organic Chemistry; Reactivity and Structure*; Springer: Heidelberg, Germany, 1987; Vol. 25.

(21) Imahori, H.; Tkachenko, N. V.; Vehmanen, V.; Tamaki, K.; Lemmetyinen, H.; Sakata, Y.; Fukuzumi, S. *J. Phys. Chem. A* **2001**, *105*, 1750.

(22) Imahori, H.; Hagiwara, K.; Aoki, M.; Akiyama, T.; Taniguchi, S.; Okada, T.; Shirakawa, M.; Sakata, Y. *J. Am. Chem. Soc.* **1996**, *118*, 11771.

(23) Gould, I. R.; Farid, S. *Acc. Chem. Res.* **1996**, *29*, 522.

(24) (a) Hilinski, E. F.; Masnovi, J. M.; Amatore, C.; Kochi, J. K.; Rentzepis, P. M. *J. Am. Chem. Soc.* **1983**, *105*, 6167. (b) Hilinski, E. F.; Masnovi, J. M.; Kochi, J. K.; Rentzepis, P. M. *J. Am. Chem. Soc.* **1984**, *106*, 8071.

(25) (a) Hubig, S. M.; Bockman, T. M.; Kochi, J. K. *J. Am. Chem. Soc.* **1996**, *118*, 3842. (b) Hubig, S. M.; Bockman, T. M.; Kochi, J. K. *J. Am. Chem. Soc.* **1997**, *119*, 2926. (c) Rathore, R.; Hubig, S. M.; Kochi, J. K. *J. Am. Chem. Soc.* **1997**, *119*, 11468. (d) Bockman, T. M.; Hubig, S. M.; Kochi, J. K. *J. Am. Chem. Soc.* **1998**, *120*, 6542. (e) Hubig, S. M.; Kochi, J. K. *J. Am. Chem. Soc.* **1999**, *121*, 1688.

(26) (a) Ojima, S.; Miyasaka, H.; Mataga, N. *J. Phys. Chem.* **1990**, *94*, 4147, 5834, 7534. (b) Asahi, T.; Ohkohchi, M.; Mataga, N. *J. Phys. Chem.* **1993**, *97*, 13132. (c) Asahi, T.; Mataga, N. *J. Phys. Chem.* **1991**, *95*, 1956.

(27) Kesti, T. J.; Tkachenko, N. V.; Vehmanen, V.; Yamada, H.; Imahori, H.; Fukuzumi, S.; Lemmetyinen, H. *J. Am. Chem. Soc.* **2002**, *124*, 8067.

(28) Perrin, D. D.; Armarego, W. L. F.; Perrin, D. R., *Purification of Laboratory Chemicals*, 4th ed.; Pergamon Press: Elmsford, NY, 1996.

(29) Imahori, H.; Tamaki, K.; Araki, Y.; Sekiguchi, Y.; Ito, O.; Sakata, Y.; Fukuzumi, S. *J. Am. Chem. Soc.* **2002**, *124*, 5165.

(30) Imahori, H.; Ozawa, S.; Ushida, K.; Takahashi, M.; Azuma, T.; Ajavakom, A.; Akiyama, T.; Hasegawa, M.; Taniguchi, S.; Okada, T.; Sakata, Y. *Bull. Chem. Soc. Jpn.* **1999**, *72*, 485.

(31) Takagi, S.; Miyamoto, T. K.; Sakai, Y. *Bull. Chem. Soc. Jpn.* **1986**, *59*, 2371.

(32) (a) Tkachenko, N. V.; Tauber, A. Y.; Grandell, D.; Hynninen, P. H.; Lemmetyinen, H. *J. Phys. Chem. A* **1999**, *103*, 3646. (b) Tkachenko, N. V.; Rantala, L.; Tauber, A. Y.; Helaja, J.; Hynninen, P. H.; Lemmetyinen, H. *J. Am. Chem. Soc.* **1999**, *121*, 9378.

(33) Mann, C. K.; Barnes, K. K. *Electrochemical Reactions in Nonaqueous Systems*; Marcel Dekker: New York, 1990.

(34) Stewart, J. J. P. *J. Comput. Chem.* **1989**, *10*, 209, 221.

(35) Fuhrhop, J.-H.; Mauzerall, D. *J. Am. Chem. Soc.* **1969**, *91*, 4174.

(36) Luo, C.; Guldi, D. M.; Imahori, H.; Tamaki, K.; Sakata, Y. *J. Am. Chem. Soc.* **2000**, *122*, 6535.

(37) (a) Akimoto, S.; Yamazaki, T.; Yamazaki, I.; Osuka, A. *Chem. Phys. Lett.* **1999**, *309*, 177. (b) Nakano, A.; Yasuda, Y.; Yamazaki, T.; Akimoto, S.; Yamazaki, I.; Miyasaka, H.; Itaya, A.; Murakami, M.; Osuka, A. *J. Phys. Chem. A* **2001**, *105*, 4822.

(38) (a) Andersson, M.; Davidsson, J.; Hammarström, L.; Korppi-Tomola, J.; Peltola, T. *J. Phys. Chem. B* **1999**, *103*, 3258. (b) Harriman, A.; Hissler, M.; Trompette, O.; Ziessel, R. *J. Am. Chem. Soc.* **1999**, *121*, 2516.

(39) Kesti, T.; Tkachenko, N.; Yamada, H.; Imahori, H.; Fukuzumi, S.; Lemmetyinen, H. *Photochem. Photobiol. Sci.* **2003**, *2*, 251.

(40) The maximum bleaching of the porphyrin ground-state absorption is achieved at 5−15 ps delay time (Figure 6). Also the 4.3 ps component (Figure 6) has a sharp band at 560 nm, which allows associating it with Q-band bleaching. Therefore, this component, 4.3 ps, can be attributed to formation of the exciplex from fullerene singlet excited state. Noticeably, this relaxation channel gives only minor absorption increase in PhCN. In toluene, its contribution is even less visible giving no observable signal increase at the same wavelengths.

(41) The extinction of the CT band is roughly 1000 times lower than that of the Soret band, which is right at the excitation wavelength. It is hardly possible to achieve any sensible amount of directly excited CT. On the other hand, relaxation of the second excited state to exciplex is an extremely fast reaction and will be observed as almost instant formation of the exciplex.

(42) (a) Fukuzumi, S.; Suenobu, T.; Patz, M.; Hirasaka, T.; Itoh, S.; Fujitsuka, M.; Ito, O. *J. Am. Chem. Soc.* **1998**, *120*, 8060. (b) Fukuzumi, S.; Suenobu, T.; Hirasaka, T.; Sakurada, N.; Arakawa, R.; Fujitsuka, M.; Ito, O. *J. Phys. Chem. A* **1999**, *103*, 5935.

(43) Imahori, H.; El-Khouly, M. E.; Fujitsuka, M.; Ito, O.; Sakata, Y.; Fukuzumi, S. *J. Phys. Chem. A* **2001**, *105*, 325.

(44) (a) Kadish, K. M.; Gao, X.; Van Caemelbecke, E.; Suenobu, T.; Fukuzumi, S. *J. Phys. Chem. A* **2000**, *104*, 3878. (b) Guldi, D. M.; Asmus, K.-D. *J. Phys. Chem. A* **1997**, *101*, 1472. (c) Guldi, D. M.; Hungerbühler, H.; Asmus, K.-D. *J. Phys. Chem.* **1995**, *99*, 9380.

(45) The third important parameter is the mutual orientation of the reactant. However, the molecular modeling (Figure 3) indicates only slight and unregular variation in the orientation factor for this series of the dyad, whereas the distance changes from almost van der Waals contact to 5.2 Å (edge-to-edge).

(46) The molecular modeling was performed for free base dyads, Figure 3. However, one can expect a similar relation in center-to-center distances for the Zn dyads.

(47) The exciplex of ZnP-D-C_{60} can be regarded as the charge-separated state with a strong interaction. However, the exact difference between the exciplex and charge-separated state remains to be clarified, although they are clearly differentiated by their transient absorption spectra as shown in this study.